*ICANS-XI International Collaboration on Advanced Neutron Sources*
*KEK, Tsukuba, October 22-26, 1990*

# SIMULTANEOUS PULSED/INTEGRAL NEUTRON FACILITY OPTIMIZATION

I.M. Thorson
*TRIUMF, 4004 Wesbrook Mall, Vancouver, B.C. V6T 2A3*

## ABSTRACT

The possibilities and compromises necessary in the design of a neutron facility that would serve both pulsed and time integral users simultaneously are examined.

## 1. INTRODUCTION

Traditionally thermal neutron beam users have divided into two, occasionally armed camps. The maximum intensity available for monochromation by Bragg reflection of the broad thermal neutron spectrum has always been found at fission reactors. Such instruments are limited to the strictly thermal neutron energy region by two factors: the decreasing reflectivity of the monochromating (and energy analysing) crystals and the lack of epithermal neutrons in the incident neutron beams. The pulsed neutron instruments using choppers to monochromate and time-of-flight for neutron energy analysis get by with much smaller integral neutron beams by phasing the choppers to the neutron source pulses. Because the source flash is brighter by factors up to 100 for thermal neutrons and more than 1000 for epithermal neutrons they are the source of choice for such instruments. The beam power available from the present accelerators that operate in a pulsed mode is approximately 100 kW. The flux available to integral beam users from a target assembly optimized for such use would be a factor ~50 less than that available from the ILL fission reactor. As the intensity gap available between accelerator sources and fission reactor sources closes the question of optimization of target assemblies for both integral and pulsed beam users becomes important.

If a neutron facility requires N different target-moderator assemblies to satisfy the various users the overall availability of their facility for *all* users is $N^{-1}$. Thus the total overall availability to any user is maximized as long as the compromises necessary in a common facility design cost less than a factor at least 2 in beam availability.

The question to be addressed then is what are the approximate intensity reduction factors to the various types of instruments that common facilities would impose.

The second section uses simple one-dimensional neutron diffusion theory to estimate the epithermal and thermal fluxes available in infinite moderator assemblies of various materials. The epithermal and thermal neutron spectral components are illustrated and their spatial and temporal variations defined. In section three some of the constraints that would be necessary in the design of a "universal" target-moderator assembly are discussed. Section

four draws general conclusions and makes some recommendations on the directions for future developments.

## 2. NEUTRON FLUX ESTIMATION

### *A. Steady State or Time Integral*

The diffusion theory approximation for the epithermal neutron flux in an infinite medium surrounding a void of radius $R$ containing a source of $S$ fast neutrons of energy $E_o$ is given by[1]

$$\phi_{\rm epi}(r) = \frac{S}{4\pi r}\frac{\lambda_s ln(E_o/E_{th})}{\xi}\frac{e^{-\frac{r-R}{L_s}}}{L_s(L_s+R)} \tag{1}$$

where $r$ is distance from the source at the center of the void, $\lambda_s$ is the transport mean-free-path, $\lambda_s = (\Sigma_s(1-\overline{\mu}))^{-1}$, $\Sigma_s$ is the macroscopic scattering cross section and $\overline{\mu}$ is the mean cosine of the scattering angle in the infinite medium material, $\xi$ is the mean logarithmic energy loss per (elastic) scattering collision, $E_{th}$ is the thermal neutron energy, ~0.026 eV at room temperature, and $L_s$ is the slowing down length

$$L_s^2 = \frac{1}{3}\int_{E_{th}}^{E_o}\frac{\lambda_s^2}{\xi(1-\overline{\mu})}\frac{dE}{E}. \tag{2}$$

Figure 1 shows the expected spatial distribution of the epithermal neutron flux for infinite media of various materials surrounding a 10 cm radius void containing a fast neutron source. The diffusion model implicitly estimates the integral over energy for a single epithermal group during the thermalization process from the intitial energy – approximately 2 MeV – to thermal, ~0.026 eV at 300° K. No neutron loss mechanism is considered except transfer to a thermal energy group at the end of the thermalization process. The neutron thermalization and diffusion parmeters shown in Table I are based on a fission reaction source spectrum; the somewhat border spectra from spallation reactions would change them only marginally. Within the epithermal group the time-averaged spectrum is expected to have an approximate $E^{-1}$ energy dependence.

For the neutrons reaching thermal energies with the distribution given by (1) above the thermal neutron flux distribution is

$$\phi_{th}(r) = \frac{S}{4\pi r}\frac{\lambda_a}{(L_s^2-L^2)}\left(\frac{L_s}{L_s+R}e^{-\frac{r-R}{L_s}} - \frac{L}{L+R}e^{-\frac{r-R}{L}}\right) \tag{3}$$

where $L$ is the thermal neutron diffusion length

$$L = (\frac{\lambda_a\lambda_t}{3})^{1/2} \tag{4}$$

$\lambda_a$ is the thermal neutron capture mean-free-path and $\lambda_t$ is the thermal neutron transport mean-free-path similar to that defined for epithermal neutrons, above. The expressions approximate both the steady state spatial distributions for continuous sources and the time-integrals for time dependent sources. It does not, however, approximate the thermal neutron spatial flux distribution immediately following thermalization, as will be discussed below.

Figure 2 shows the expected time-averaged thermal neutron flux distribution for the thermalized source distributions shown in Fig. 1 for the various infinite media. The estimate

**Table I**
Neutron Thermalization and Diffusion Parameters

| | $H_2O$ | $D_2O$ (H/D=0.002) | Be ($\rho$=1.7 g cm$^{-3}$) | C ($\rho$ = 1.8 g cm$^{-3}$) | Fe | Ni | Pb |
|---|---|---|---|---|---|---|---|
| $\lambda_{a,cm}$ | 45 | 11,300 | 960 | 3260 | 4.6 | 2.5 | 178 |
| $\lambda_{t,cm}$ | 0.49 | 2.60 | 1.60 | 2.5 | 1.1 | 0.63 | 2.7 |
| $L_{,cm}$ | 2.7 | 99 | 22.6 | 52 | 1.3 | 0.72 | 12.6 |
| $\lambda_{s,cm}$ | 0.67 | 2.82 | 1.43 | 2.33 | 1.4 | 0.76 | 2.9 |
| $L_{s,cm}$ | 5.5 | 11.0 | 9.3 | 18.7 | 18.5 | 10.4 | 74 |
| $\xi$ | 0.925 | 0.509 | 0.209 | 0.158 | 0.0354 | 0.0337 | 0.0096 |
| $\lambda_s/\xi\lambda_a$ | $16\times10^{-3}$ | $0.49\times10^{-3}$ | $7.1\times10^{-3}$ | $4.5\times10^{-3}$ | 8.6 | 9.4 | 1.7 |

$\lambda_a$ – capture mean-free-path for thermal neutrons, based on 2200 m s$^{-1}$ cross sections and Westcott convention flux.

$\lambda_t$ – transport mean-free-path for thermal neutrons, $= (\Sigma_s(1-\overline{\mu}))^{-1}$, where $\Sigma_s$ is macroscopic scattering cross section and $\overline{\mu}$ is the average cosine of the scattering angle.

L – thermal neutron diffusion length, $= (\frac{\lambda_t\lambda_a}{3})^{1/2}$.

$\lambda_s$ – scattering mean-free-path for epithermal neutrons.

$L_s$ – neutron slowing down length, from $E_0$ to $E_{th}$, $L_s^2 = \frac{1}{3}\int_{E_{th}}^{E_0} \frac{\lambda_s^2}{\xi(1-\overline{\mu}_s)}\frac{dE}{E}$, $E_0 \approx 2$ MeV

$\xi$ – mean logarithmic energy loss per scattering collision, $\xi \approx 2/(A+\frac{2}{3})$, A is atomic weight.

uses the experimental neutron diffusion parameters from Table I for the common moderators based on measurements with fission-neutron spectra[2]. They are expected to be a reasonable approximation to the distribution around a lightly absorbing target and container (lead in zirconium, for example). The estimated thermal neutron flux in the vicinity of the target edge is the same, within a factor 2, for all of the better moderator materials. The ratio of the epithermal/thermal flux is given by

$$\frac{\phi_{\rm epi}(r)}{\phi_{th}(r)} = \frac{\lambda_s ln(E_o/E_{th})}{\xi\lambda_a} \times \frac{L_s^2 - L^2}{L_s^2 - L_s L(L_s+R)/(L+R)e^{-\frac{L_s-L}{L_s L}(r-R)}} \cdot \qquad (5)$$

For $L > L_s$ this ratio decreases with increasing distance from the source, as is shown in Fig. 3. For $L_s > L$ this ratio becomes constant as the second term in the denominator vanishes, as for $H_2O$. The factor $\lambda_s/\xi\lambda_a$ is the ratio between the $E^{-1}$ epithermal neutron spectrum and the thermal, Maxwellian neutron spectrum in an infinite medium with a uniformly distributed source of fast neutrons. Such spectra are shown in Fig. 4, transformed to constant reciprocal velocity, $\tau$, interval after extracting a factor $\tau$ from the denominator. The curves as shown are proportional to the intensity seen by a time-of-flight or a perfect Bragg-reflection spectrometer for a fixed fractional velocity or reflection-angle resolution. The thermal neutron spectra for three different Maxwellian temperature are shown. The slowing-down spectra normalizations are those for uniform infinite media sources. The neutron energy, $E_n$, as the function of neutron reciprocal velocity, $\tau$,

$$E_n = 5213\ \tau^{-2} \qquad (6)$$

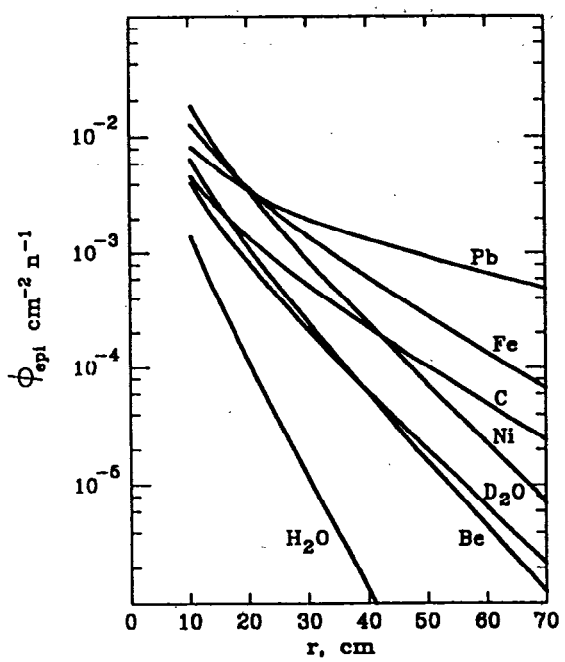


Fig. 1. The one-dimensional diffusion theory estimate of the epithermal neutron flux distribution in infinite media of various materials outside a 10 cm radius void are shown normalized to unit neutron source strength using the thermalization and diffusion parameters from Table I.

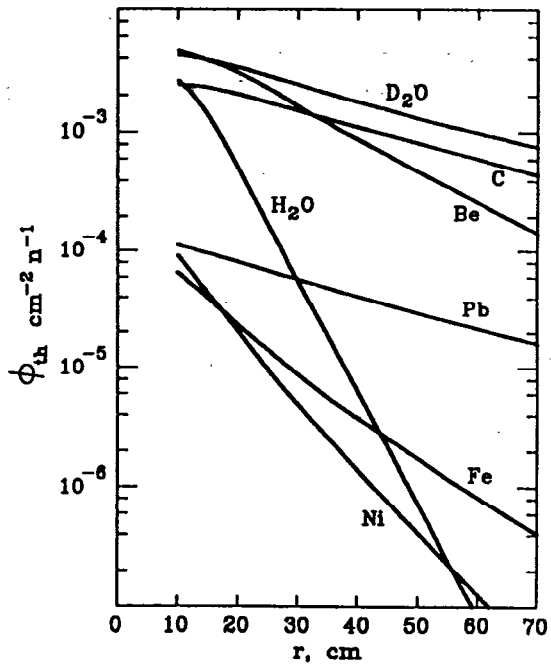


Fig. 2. The thermal neutron flux distributions are shown for the epithermal source distributions and geometry of Fig. 1.

$E_n$ in eV, $\tau$ in $\mu$s m$^{-1}$, is also shown on Fig. 4. The normalization of the results in Fig. 3 is the same as for Fig. 4, i.e. the dotted lines in Fig. 4. representing the levels of the epithermal spectra in various materials track as functions of positions according to the results in Fig. 3. The dotted curve in Fig. 3 indicates the level of the (constant with temperature) maxima in the Maxwellian (thermal neutron) spectra, which can then be renormalized by the spatial distributions shown in Fig. 2.

*B. Pulsed Neutron Sources*

Table II shows the mean lifetimes for thermal and epithermal neutrons in the same infinite media for which the spatial distributions were estimated above. The thermal neutron lifetime is simply the quotient of the mean-free-path to capture divided by the mean neutron velocity, $v_t = 2.5 \times 10^3$ m s$^{-1}$ for a room-temperature Maxwellian. The thermal neutron lifetimes can of course be shortened in an infinite medium only by adding absorber to the system, with a proportionate decrease in the time-integral thermal neutron flux. For moderators of finite size the relaxation rate is increased by leakage according to[3]

$$\phi_{th}(t) = \phi_o e^{-\lambda t} \tag{7}$$

where

$$\lambda \approx \alpha + DB^2 \tag{8}$$

and $\alpha = v_t \lambda_a^{-1}$ is due to neutron absorption as in the infinite system,
$B^2 = (\pi/r)^2$ for sphere of radius r,
$= (\pi/h)^2 + (2.405/r)^2$ for a cylinder of radius $r$ and height $h$,
$= (\pi/a)^2 + (\pi/b)^2 + (\pi/c)^2$ for a parallelepiped of sides $a, b$ and $c$.
$D = v\lambda_t/3$ is the diffusion constant for neutrons leaking out of the system,

($B$ is the geometrical buckling in the vernacular of fission reactor physics.)

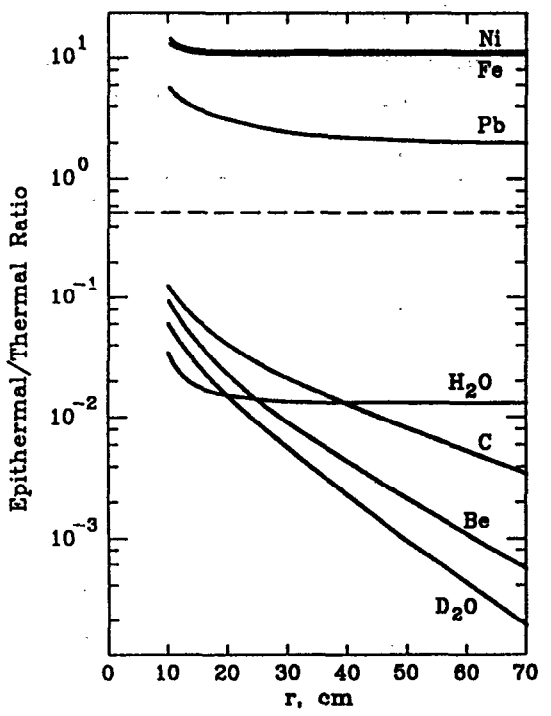


Fig. 3. The ratio of epithermal/thermal neutron fluxes are shown for the same systems and approximations as Figs. 1 and 2. (See text for normalization details).

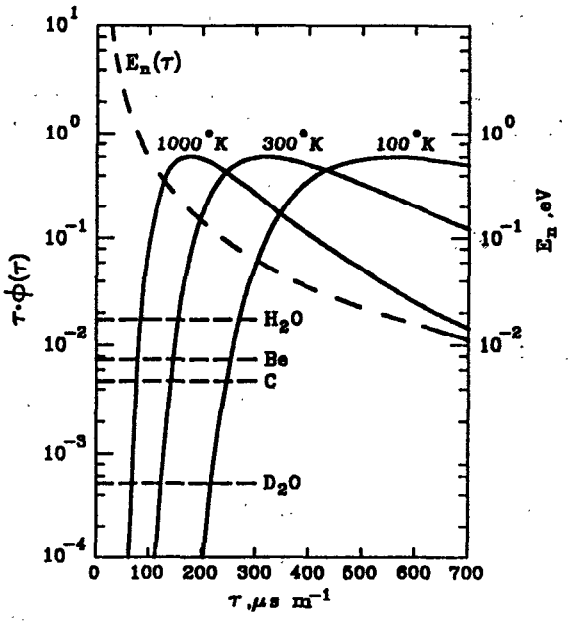


Fig. 4. The thermal and epithermal neutron spectra for infinite media with uniformly distributed sources of fast neutrons are shown for the common moderators. The spectra are shown as the functions $\tau \cdot \phi(\tau)$ where $\tau$ is the neutron reciprocal velocity (in $\mu s\ m^{-1}$) and $\phi(\tau)$ is the distribution per unit reciprocal velocity interval.

This expression for $\phi_{th}(t)$ is an approximation, the conditions for which are seldom, if ever, well satisfied and may not be valid for all systems of interest. In particular, heterogeneous systems of different materials may 'store' neutrons in regions with longer neutron slowing-down delays or thermal neutron lifetimes and feed them back to regions that would otherwise be more quickly populated or depleted. Thus, simple, single time-constant exponential thermalization and decay may not always be an adequate approximation for all neutron histories of interest.

Ikeda and Carpenter (ref 4) have shown experimentally that for typical compact hydrogenous moderator systems, the neutron leakage pulse at a particular neutron energy in the thermal region reqires two terms:

$$\chi(a,\beta,R,t) = \frac{a}{2}\left\{(1-R)(at)^2 e^{-at} + 2\frac{Ra^2\beta}{(a-\beta)^3} \times \left[e^{-\beta t} - e^{-at}\left(1 + (a-\beta)t + \frac{1}{2}(a-\beta)^2 t^2\right)\right]\right\} \quad (9)$$

where $a$ = $v\xi\Sigma_s$, defines the transferrate from the epithermal to the thermal group
$\beta$ = time constant for thermal neutron loss from system, and
$R$ = fractional yield in the thermal neutron term.

The first term represents the thermalization component that decays fairly quickly even at thermal neutron energies; the second term comes from the equilibrium thermal neutron component that has a nominal time constant of the order of $\beta = \lambda$ from Eq. (8). The thermal component weighting $R$ value depends on the Maxwellian amplitude at the energy of interest as well as thermalization characteristics of the system. In practice it is an empirically derived parameter extrapolated from systems of a similar configuration and moderator characteristics.

**Table II**
Thermal and Epithermal Neutron Lifetimes

| Material | $\gamma$ | $\bar{t}_{th}$ | $\bar{t}_s$ (to 1 eV) | $\Delta\bar{t}_s$ (to 1 eV) |
|---|---|---|---|---|
| | | $\mu$s | $\mu$s | $\mu$s |
| $H_2O$ | 0.99 | 180 | 1.7 | 2.0 |
| $D_2O$ | 0.56 | $45\times10^3$ | 4.8 | 4.7 |
| (H/D=0.002) | | | | |
| Be | 0.148 | $3.8\times10^3$ | 7.9 | 4.7 |
| ($\rho$ = 1.7 g cm$^{-3}$) | | | | |
| C | 0.111 | $13\times10^3$ | 20.2 | 10.8 |
| ($\rho$ = 1.8 g cm$^{-3}$) | | | | |
| Fe | 0.0239 | 18 | 58 | 14.8 |
| Ni | 0.0227 | 10 | 34 | 8.5 |
| Pb | 0.0064 | 710 | 440 | 59 |

$\bar{t}_{th}$ – average thermal neutron lifetime.
$\bar{t}_s$ – average thermalization time.
$\Delta\bar{t}_s$ – full-width, half-maximum of thermalization distribution.
$\gamma$ – thermalization parameter, $\approx 4/(3A)$ in $\bar{t}_s = (1+2/\gamma)(\gamma\lambda_s/\xi v)$
and $\Delta t_s = 2.35(1+2/\gamma)^{\frac{1}{2}}(\gamma\lambda_s/\xi v)$
where $v$ is final neutron velocity of interest.

The epithermal neutron lifetimes, $\bar{t}_s$, are also listed in Table II for the various materials. Because of the relatively narrow fractional range of the initial energies of most of the source neutrons and the close correlation between time and energy loss, the parameter that defines the pulse length and amplitude for homogeneous systems is the straggle width of thermalization time, also shown in Table II as $\Delta\bar{t}_s$, the full-width at half-maximum, taken from reference 3 for the light moderators and estimated from the expression listed in the footnotes of Table II for the others. Except in circumstances where significant cross-feeding of neutrons takes place between regions of different thermalization times the pulse length and amplitude is controlled by the time-straggle width and the thermalization time only introduces a phase shift in the pulse cycle.
The peak fluxes, both epithermal and thermal, that contribute beam over the short periods – a few $\mu$s – sampled by time-of-flight monochrometers are then enhanced, relative to those shown for the steady state in Fig. 1 by a peak enhancement factor ($F_{PE}$) given by

$$F_{PE} = \frac{\tau_P/\tau_L}{1-e^{-\tau_P/\tau_L}} \tag{10}$$

where $\tau_P$ is the pulse repetition period and $\tau_L$ is the mean neutron lifetime as a thermal ($\tau_L = \bar{t}_{th}$) or epithermal ($\tau_L = \Delta\bar{t}_s$) neutron as listed in Table II for infinite systems. The mean neutron lifetimes in finite assemblies can, of course, be significantly shorter than those shown in Table II but the time-integral fluxes will be reduced by the same factor leaving the initial peak fluxes constant.
There is however another factor that must be considered in estimating the thermal neutron pulse intensity available from large moderator assemblies, namely the evolution of the thermal neutron spatial

## Table III

Epithermal and Thermal Pulse Enhancement Factors for Pulse Repetition Period of 20 ms

| Material | $F^*_{PE}$ (epithermal)[1] (to 0.026 eV) | $F^*_{PE}$ (thermal)[2] (short time) | $F_{PE}$ (thermal)[3] (long time) |
|---|---|---|---|
| $H_2O$ | 1600 | 1500 | 110 |
| $D_2O$ | 690 | 560 | 1.2 |
| Be | 690 | 620 | 5.3 |
| C | 300 | 270 | 2.0 |
| Fe | 220 | 220 | 1100 |
| Ni | 380 | 380 | 2000 |
| Pb | 55 | 55 | 28 |

1) $\tau_L = \overline{\Delta t_s}/(0.026)^{1/2}$
2) $\tau_L = ((\overline{\Delta t_s}/0.026)^2 + (\frac{\lambda_t}{3v})^2)^{\frac{1}{2}}$
3) $\tau_L = \bar{t}_{th}$

distribution with time. At thermalization the spatial distributions of the neutrons are essentially those shown in Fig. 1 for epithermal neutrons in various materials. These distributions evolve with time to give the time-integral distributions shown in Fig. 2. The pulse enhancement factor thus depends on position within the moderator, especially for materials where L>$L_s$. The asymptotic limits for the effective lifetimes are the reciprocals of the neutron capture rate at long time ($\bar{t}_{th}$ in Table II) and the reciprocals of the neutron diffusion rates ($\tau_L = \lambda_t(3v_t)^{-1}$) at short distances and short times. At short times the diffusion rates are comparable to the thermalization rates and the effective pulse enhancement factors are similar to those for the epithermal components, as shown in the last column of Table III. Thus the dominant contribution to the peak pulse intensity at all energies near the source in large moderator assemblies comes from the epithermal or recently thermalized component. Because the epithermal fluxes decrease rapidly with radial distance from the source as shown in Fig. 1, all beam tubes for such pulsed beams must penetrate to positions near the target. At these short distances, however, the three best moderators, $H_2O$, $D_2O$ and Be, all give similar peak pulse intensities for both epithermal and thermal energies. The time integral intensities are also comparable for neutron source positions near the target; the Be or $D_2O$ moderators would, however, allow geometries much less congested than for $H_2O$. Large all-nickel and iron moderators would also yield very good peak epithermal fluxes but would give very poor integral thermal neutron fluxes.

The time-integral thermal neutron flux is always maximum in a large $D_2O$ moderator assembly, as reiterated by the results in Fig. 2. Its dependence on distance from target is weak enough that thermal neutron beam tubes can be terminated at least 30 cm from the target centre without suffering intensity penalties more than a factor 2. This allows off-setting of the beam tubes to tangential geometry and ahead of target entry point of the proton beam to minimize fast neutron contamination that usually dominates the background problem for most experimental instruments. To maximize the thermal neutron flux, however, the moderator, target and structural components must have minimum neutron capture cross-section.

No substantial intensity penalties are expected for either integral and pulsed neutron beam of all energies if the additional constraint of short neutron lifetimes applied to the present PNF designs is removed.

## 3. DESIGN CONSTRAINTS FOR OPTIMUM PULSED/INTEGRAL NEUTRON FACILITIES

The constraint of minimum absorption or leakage in small moderator assemblies to achieve optimum integral thermal neutron beams requires that all time-of-flight monochromotors include a second phased beam chopper in the vicinity of the target moderator assembly. This will be quite an acceptable price where (and when) the accelerators have power levels large enough to compete with the fission reactors. A $10^{15}$ $cm^{-2}$ $s^{-1}$ thermal neutron flux requires approximately 6 MW of beam power at approximately 1 GeV proton energy. The beam power from the KAON accelerators approaches this level but at an energy that is probably too high for optimum neutron source production.
The second over-riding constraint for a high power facility will be heat dissipation in the target. Given the intensity incentive implied by Fig. 1 for compact sources only pumped liquid metal targets are likely to be capable of the several MW per liter heat dissipation required. Fortunately both lead and bismuth, the most probable materials, are not heavy thermal neutron absorbers.

## 4. CONCLUSION

It appears that no fundamental neutronic constraints preclude simultaneous optimization of the integral and pulsed neutron beams available from an accelerator based neutron facility. The simple single phased chopper monochromation systems presently employed at such facilities must, however, be augmented by second phased chopper as were originally used on fission reactors more than 30 years ago[5].

## REFERENCES


[1] P.R. Wallace and J. LeCaine, *Elementary Approximations in the Theory of Neutron Diffusion*, Chalk River Nuclear Laboratory report AECL No. 336, 1943.

[2] ANL-5800 *Argonne National Laboratory Reactor Physics Constants*, Second Edition, 1963.

[3] J.M. Carpenter, *Pulsed Spallation Neutron Sources for Slow Neutron Scattering*, Nucl. Instrum. and Meth. 145 (1977) pp 91-113.

[4] S. Ikeda and J.M. Carpenter, Nucl. Instrum. and Meth. A239 (1985) p 536.

[5] P.A. Egelstaff *et al.*, *A Four-Rotor Thermal Neutron Analyzer, Inelastic Scattering of Neutrons in Solids and Liquids*, IAEA, Vienna (1961) p 165.